Journal of ICT, Design, Engineering and Technological Science (JITDETS)
VOL. 5, NO. 1, pp. 1-8, 2021
DOI: https://doi.org/10.33150/JITDETS-5.1.1

ORIGINAL CONTRIBUTION

An Analysis of Geometrical and Failure Characteristics of Laser Micro-Welded SS304 and DSS2205

R. M. Mithun[1], M. M. Quazi[2*], M. Nasir Bashir[3], M. Ishak[4], M. H. Aiman[5]

[1,2,4,5] Joining, Welding and Laser Processing Lab (JWL), Faculty of Mechanical and Automotive Engineering Technology, University Malaysia Pahang, Pekan, Pahang, Malaysia

[3] National University of Sciences and Technology (NUST), Islamabad, Pakistan

***Abstract*— Laser micro-welding is being widely used in many industries because of its speed and precision. This study's Stainless Steel (SS304) and Duplex Stainless Steel (DSS 2205) possess good ductility and strength. However, laser micro-welding is a challenge for joining dissimilar materials. Pulse wave mode micro-welding was employed in this study. The parameters that were varied throughout the study were the peak power and hatching distance. With that being so, the other parameters such as frequency, pulse width, mark loop and welding speed were kept constant. After preliminary tests were carried out, a range of parameters was obtained by knowing the threshold value to obtain a proper joint. The welded specimens were analyzed by conducting weld geometrical properties analysis, failure analysis with the aid of image analysis software (Image J), and surface color examination. The strongest tensile strength value obtained was 13.56 MPa with a weld width of 0.611mm, whereas the least tensile strength value was 0.8 MPa with a weld width of 0.577mm. A percentage difference of 177.015% between the highest and lowest tensile stress value was observed. The highest distortion lies with specimen I (power 95%, hatching distance 0.001mm) with an angular deviation of 5.013° on the left side and 4.086° on the right concerning the horizontal place. It was concluded that too high power caused distortion, thereby resulting in a poor joint.**

***Index Terms*— Laser Micro-welding, SS304, DSS2205, Failure Analysis, Colour Analysis**

Received: 21 February 2021; **Accepted:** 15 April 2021; **Published:** 08 June 2021

I. INTRODUCTION

In this era of technology, the welding process can be performed in many different methods and techniques. Welding is defined as the process of joining two similar or dissimilar materials by applying heat to soften and melt the materials while allowing them to cool down, subsequently ensuing in the fusion of materials. Welding is now a commonly used method to join materials, as its ability to weld complex structures, high strength of joint specimens, cheap and highly reliable [1]. Welding can be categorized into two, which are solid-state welding and fusion welding. In solid-state welding, materials are not melted to form a molten pool. In contrast, infusion state welding, the melting of material to form a molten pool to join the materials, occurs. Diffusion welding, cold welding, friction welding and resistance welding are several types of solid-state welding. There are also relatively newer techniques such as laser welding [2], and to carry out welding for components in micrometers size, laser micro-welding is employed [3]. The efficacy of a technology depends on the link resistance and its scatter, and the particular joining task [4].

Laser micro-welding is a non-contact non-wear approach that does not require pre-treatment of the surface and is not limited to certain materials, offering many advantages compared to traditional methods: higher process speed, a high degree of automation, no added material and a link locking material [5]. It is possible to understand the scaling effects that strictly affect welding efficiencies, such as solidification structure, cooling rate, distortion, surface tension and fluid flow stability [6]. Besides, some significant laser variables such as the beam diameter, laser strength, travel speed, beam configuration, substrate state, thermo physical properties of the work piece, and the alloy's composition affect laser micro-welding [7, 8]. In cases where the features of micro-machining can be reduced to micro-scales in size, micro-welding is an efficient technique for the production process [9].

In contrast to macro-range industrial manufacturing processes, the laser micro-welding joining technique has a high rating in microsystems technology and biomedical applications [10, 11]. Thin metal sheets have shown a very sensitive response to heat input in the weld bead, and the geometry of the weld bead plays an important role in the joining strength. In thin metal sheet welding, conventional techniques face some difficulties, such as some blowholes created in the weld bead because of extreme heat input [12]. Thus, economically and technically, heat input minimization to thin sheet metal is too important [13]. Less heat input requires lower laser power from an economic point of view, resulting in low running costs and small investments in equipment. Less heat input, less Heat Affected Zone (HAZ) and finally little material loss due to evaporation ends up technically [9]. Precise control of heat input is possible in laser welding due to

*Corresponding author: M. M. Quazi
†Email: moinuddin@ump.edu.my

the pulse wave mode effect [14].

[15] carried out micro welding for battery applications and fuel cells using fiber lasers of 450 nm wavelength. It was found that as the wavelength decreases, the absorptivity increases. Further to this, scanning speed plays an important role in oxidation rates. [16] employed Ni interlayer to enhance the welding characteristics of NiTiNb/Ti6Al4V dissimilar material. Fracture strength of 122N was obtained. Das et al. [17] carried out micro foil welding of 200 microns of AISI 316L steel and carried out lap shear and T-peel strength analysis. Welding speed was the main parameter that was varied, and it was found that no cracks or porosity was found, and the amount of spatter was minimum. Venkatesu et al. [18] made a comparison of High-temperature Brazing (HTB), Gas Tungsten Arc Welding (GTAW) and laser beam welding. It was determined that laser welding exhibited better mechanical properties than GTAW and HTB joints. Recently laser keyhole micro-welding of aluminum foils to lap joints having gap sizes greater than 80 percent of the foil thickness [19].

The aforementioned shows that laser micro-welding of thin foils is relatively a new process that is being significantly studied. Laser micro-welding can be carried out by a laser surface marking/modification machine with the help of a hatching parameter. Here, in this study laser marking machine is employed to carry micro-welding at very lower power levels. However, welding properties are highly affected in laser micro-welding, such as speed, power, frequency and penetration depth. To overcome this issue, in this research, the authors will carry out laser micro-welding for SS304 alloy and determine the relationship between laser properties and weld properties. Additionally, in this study, identifying the more significant parameters for laser micro-welding will be examined.

II. EXPERIMENT SETUP

A. Material Preparation

In this study, the thickness of duplex stainless steel was 2 mm, whereas the thickness of SS304 stainless steel was 0.1 mm. The composition of the materials was obtained using the Foundry Master spectrometer. Both the metals were aligned in joint lap configuration for the welding process, as shown in Fig. 1. The stainless steel is cut into the desired dimension using a hand grinder. Then, surface cleaning using acetone on SS-304 stainless steel to remove the surface coating and edges removal on both materials A jig was used to clamp the 2 metals in place with a distance of 10mm lap joint overlap. Mechanical research performed in this study is the tensile test. Joint strength can be derived from the ultimate tensile strength. The tensile test results in fracture, elongation and strength of the workpiece.

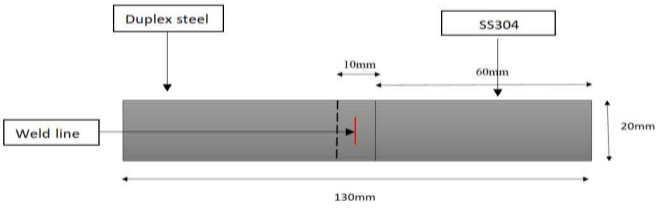

Fig. 1. Schematic diagram of the welded specimen

B. Laser Micro-welding Setup

The whole laser welding process is carried out using IPG YLM 200/2000 – QCW Fibre laser machine as shown in Fig. 2. This machine can do laser welding in both CW mode and PW mode. The maximum mean power in the continuous wave function is 0.02 kW, whereas the peak power of the pulse wave function is 0.2 kW. But in the pulse wave function, the duty cycle of the machine is not exceeding 10%. The cross-section of the bead on the plate shows the penetration of pulse wave mode is deeper than continuous wave mode for the same average power used. The light is transferred to the laser head via a fiber-optic and collimator point. The focus lens is fixed at the head of the laser and is shielded by a protective mirror. The disparity between laser focal lens and focus spot is 200 mm. A computer is installed with its respective software for the welding parameters to be inserted. A custom welding jig is used to make the welding process easier. Although the welding process only performs in the x-axis, the z-axis is additionally significant for different scopes of major length alteration, likewise to the formation of the y-axis for arrangement. The shielding gas is pumped by a custom-made side-blown design of a 6 mm copper nozzle. The distance and angle of the shielding gas will differ based on the specifications of the experiment. To reduce plasma plume formation above the keyhole, the optimization of shielding gas parameters is a must. Optimum plasma suppression can be achieved with the blowing angle of shielding gas below 30°. Plasma size decreases as the gas flow rate increases without affecting the stability of the Keyhole (k5). Gas flow rate is important in producing high-quality welding, especially when using low power laser, which requires slow welding speed. Thus, 20° of shielding gas nozzle with a gas flow rate of 12L/s of nitrogen gas is used in this experiment. Additional analysis was carried out by Image J, software for image processing based on Java developed at the National Institutes of Health and the Optical and Computational Instrumentation Laboratory.

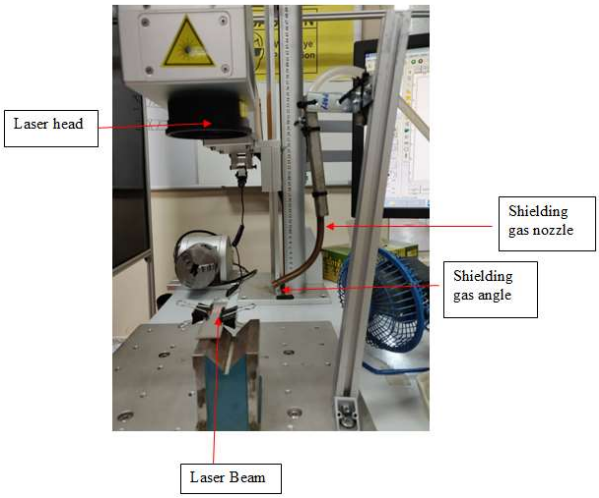

Fig. 2. IPG YLM 200/2000 – QCW Fibre laser machine for the welding process

III. RESULTS AND DISCUSSION

A. Weld Geometrical Properties Analysis

Fig. 3 shows the overview of the welded specimens that failed after tensile testing arranged in alphabetic order from bottom to top. SS304 material is arranged in the left column 4 while DSS2205 is arranged in the right column. After conducting the laser micro-welding experiment, a tensile test was conducted using the welded specimens. The Ultimate Tensile Strength (UTS) value is used to deduce the weld geometry to determine the best weld strength. Each set of experiments were repeated 3 times, and the average value obtained is used as the UTS value. Fig. 4 shows the stress-strain curve for the second trial obtained from the tensile testing. Based on the tensile test conducted from Table I, specimen B has the best average tensile strength value at tensile stress, which is at 13.45 MPa. Specimen B for DSS2205 and SS304 material is shown in Table II. The parameter combination used for this particular sample was 85% of peak power and 0.003 mm of hatching size. A sample obtained the worst tensile strength reading

I, which had a tensile strength of 0.82 MPa. The specimen I for DSS2205 and SS304 material is shown in Table III. The parameter combination for this specimen was 95% of peak power and 0.001 mm of hatching size. All specimens fractured at their respective yield strength. The sample I has the highest peak power and smallest hatching size. According to the author's work [10], higher peak power leads to spattering and underfills. Thus, with that being so, it explains why sample I has the lowest tensile strength. This is because the sample I has undergone thermal distortion. Higher pulse energy and pulse duration lead to a greater melting ratio [12, 13]. Therefore, it is important to use a suitable combination of parameters to avoid thermal distortion and defects such as spattering and underfills. Sample B has the best tensile strength of all samples because the combination of parameters gave the best joining strength. Hence the influence of the three parameters on the welded specimens has been shown in Fig. 5.

Fig. 3. Welded specimen arranged in alphabetical order from bottom to top after tensile testing

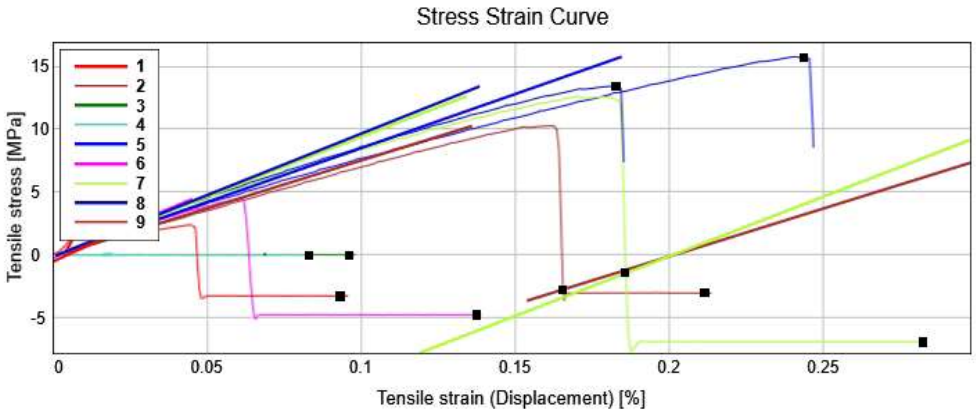

Fig. 4. Stress-strain curve of welded specimens

TABLE I
TENSILE STRENGTH AT TENSILE STRESS RESULTS

Specimen	Power (%)	Hatching Size (mm)	Tensile Strength (MPa)			Average value
			1st Set	2nd Set	3rd Set	
A/1	85	0.005	10.49	5.48	0.56	5.51
B/2	85	0.003	14.09	10.26	16	13.45
C/3	85	0.001	5.98	0.01	7.65	4.55
D/4	90	0.005	12.44	0.01	1.73	4.73
E/5	90	0.003	0.35	15.77	12.37	9.5
F/6	90	0.001	4.54	4.41	2.98	3.98
G/7	95	0.005	12.41	12.64	3.99	9.68
H/8	95	0.003	3.50	13.41	13.9	10.27
I/9	95	0.001	0.08	2.37	0	0.82

TABLE II
OPTICAL IMAGES OF SPECIMEN B OF BOTH DSS2205 AND SS304

Specimen	DSS2205	SS304
B	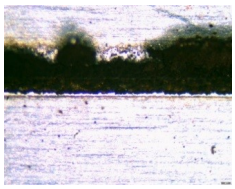	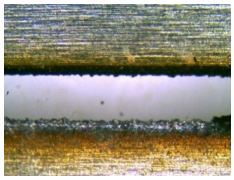

TABLE III
OPTICAL IMAGES OF SPECIMEN I OF BOTH DSS2205 AND SS304

Specimen	DSS2205	SS304
I (Zoomed)	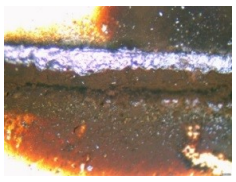	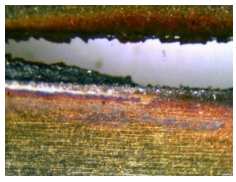

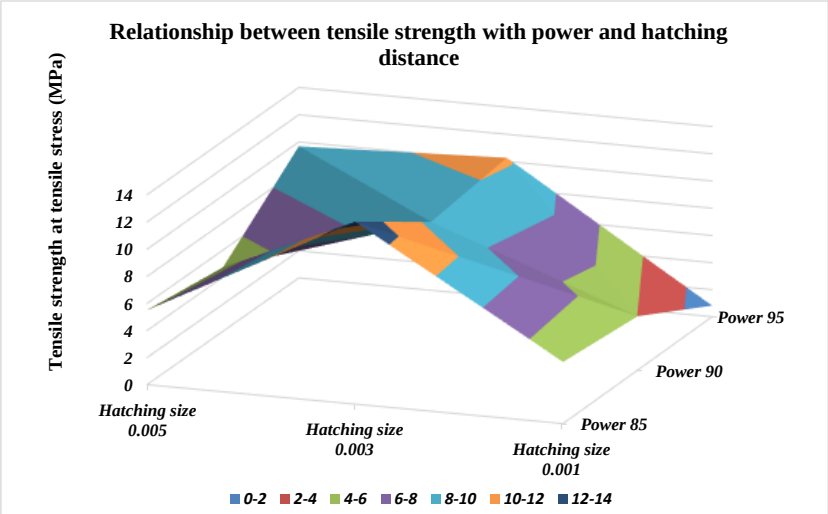

Fig. 5. Relationship of power, hatching distance and tensile strength at tensile stress

B. Surface Color Analysis

According to Table IV, color analysis can help us to utilize visual testing. The more the black area there is, the more burning is occurred and has the least tensile strength. The widest weld width was observed in sample H, whereby the weld width is 0.759 mm. The smallest weld width was observed in sample D with a width of 0.506 mm. The weld width increases with decreasing hatching size while the power is kept constant. This is simply because a narrower hatching distance allows more heat energy to pass through, eventually increasing the heat-affected zone.

TABLE IV
CONTINUATION COLOR ANALYSIS OF EACH SAMPLE

Sample	Hatching Distance (mm)	Parameters	DSS Side		SS304 Side	
			Upper Lips	Lower Lips	Upper Lips	Lower Lips
A	0.005	Power: 85% Tensile strength: 5.51 MPa	Silverish molten melted is visible	Silverish molten melted	Silverish molten melted	The transition from orange to green color
B	0.003	Power: 85% Tensile strength: 13.45 MPa	Black welded area with slight distortion and silverish molten melted	Silverish molten melted	The transition from black to green	Silverish molten melted with the transition of silver to orange
C	0.001	Power: 85% Tensile strength: 4.55 MPa	The transition of silver to green colo r	The transition of black to orange colo r	The transition from black to orange to green	The transition of silver to a mixture of green and orange
D	0.005	Power: 90% Tensile strength: 4.73 MPa	Black welded area with slight distortion and silverish molten melted	Silverish molten melted	The transition of silver to a mixture of green and orange	The transition of silver to a mixture of green and orange
E	0.003	Power: 90% Tensile strength: 9.50 MPa	Silverish molten melted	Silverish molten melted	The transition of black to a mixture of green and orange	The transition of silver to a mixture of green and orange
F	0.001	Power: 90% Tensile strength: 3.98 MPa	Silverish molten melted	The transition from silver to a mixture of orange and green	The transition of black to a mixture of green	A transition of silver to green
G	0.005	Power: 95% Tensile strength: 9.68 MPa	Silverish molten melted	Silverish molten melted with a mixture of orange	The transition of black to a mixture of green and orange	The transition of silver to orange to green
H	0.003	Power: 95% Tensile strength: 10.27 MPa	Silverish molten melted	Silverish molten melted	The transition of black to a mixture of green and orange	Silverish molten melted with the transition of silver to orange to green
I	0.001	Power: 95% Tensile strength: 0.82 MPa	Silverish molten melted is visible with a burnt orange mark	Orange burnt mark	The transition of silver to a mixture of green and orange	The transition of black to orange to green

C. Failure Analysis with Image J

The welded specimens were digitally and manually observed and analyzed using the image analysis software (Image J) for the failure after the welding process. Based on Fig. 6, the weld width varies according to different power output and hatching sizes. The Figures show that with decreasing hatching distance, the black area on SS304 increases and decreases with increasing power. The overall joint had more melting and less burning. This is observed due to the more silver area visible around and on the specimen.

The overall weld area is high with a uniform spread of color transition. The least strength is observed at the biggest black area present. And higher strength is observed at the highest silver area. Using the image j analysis software, the distortion angle of the DSS2205 material was calculated and analyzed, as shown in Table V.

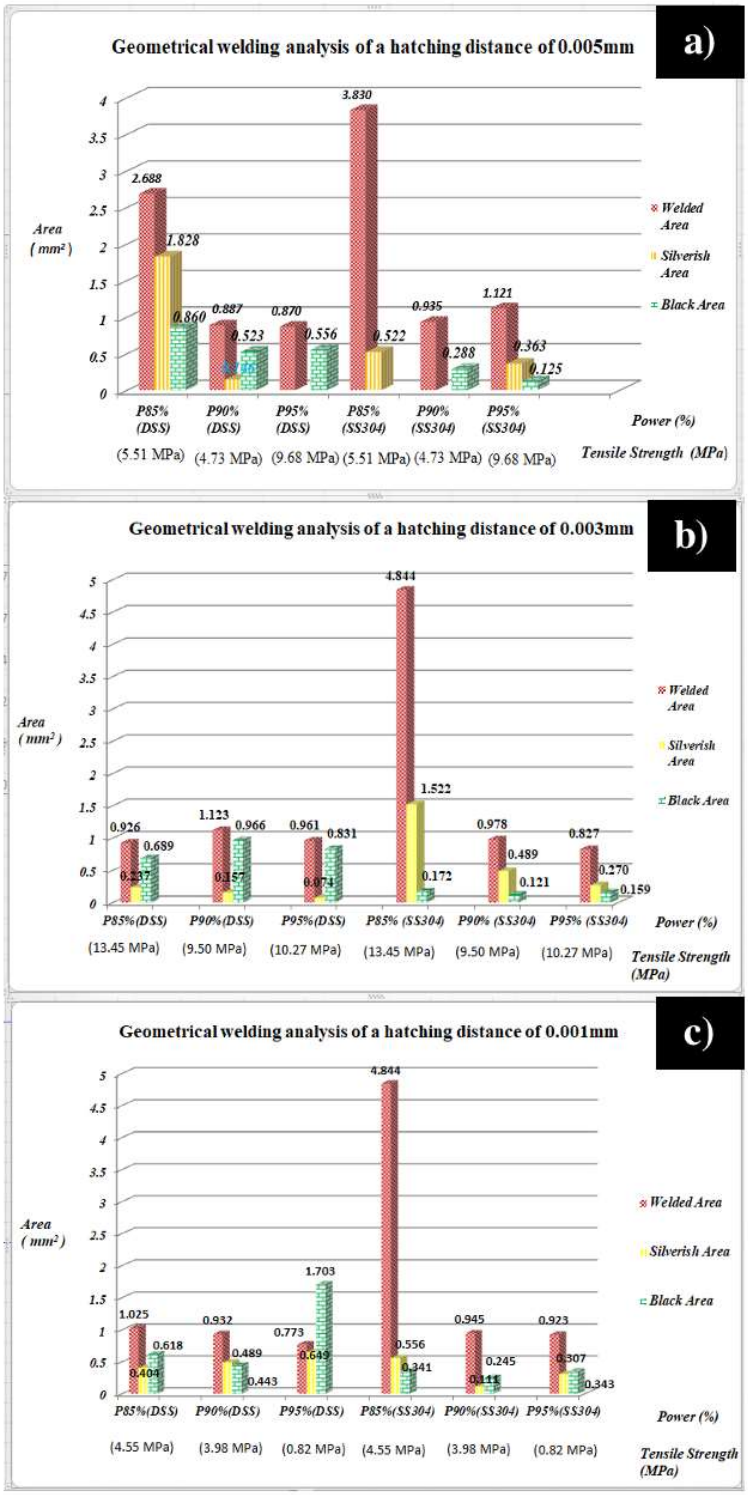

Fig. 6. Histogram of welded area, silverish area and black area at hatching distance of (a) 0.001mm (b) 0.003mm (c) 0.005mm

TABLE V
DISTORTION ANGLE OF LASER MICRO WELDED SPECIMEN

Specimen		Power (%)	Hatching size (mm)	Maximum Angle (Degree°)	Distortion
				Left	Right
A/1		85	0.005	3.245	2.444
B/2		85	0.003	4.879	4.635
C/3	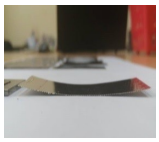	85	0.001	3.427	3.406
D/4		90	0.005	2.586	1.332
E/5		90	0.003	2.921	3.180
F/6		90	0.001	1.818	1.252
G/7		95	0.005	2.883	4.044
H/8		95	0.003	1.332	1.020
I/9		95	0.001	5.013	4.086

As reported in another research [14], laser-based micro-scale welding is a settled joining process in the advancement of smaller scale frameworks. Even though laser welding is better in productivity than most conventional, it establishes a warm process despite everything. Radiated laser vitality is especially consumed by the specimen and dissolves in that. The bit of retained energy that warms up, thus liquefying the material, is the actual welding energy. While warming up the lighted material, assimilated energy is disseminated by heat conduction misfortunes. This results in heat prompted bends in the welding specimen. Therefore, a gap evolves beneath the two specimens that are in the joint lap configuration. When the thickness at the join diminishes, the distortion similarly increases, resulting in the gap increasing. In lap welding, the maximum penetration ratio is related to the multiplied sheet thickness. The proportion of space to enable 100% entrance penetration influences weldability. This prompts diminishing weldability as sheet thicknesses decline. To help further scale down micro-scale frameworks and the welding innovation required, the mutilation brought about by dispersal misfortunes must be limited. Hence, it is recommended to increase the process efficiency of laser-based micro-welding.

In another work [15] of welding of 50 µm of SUS304H foils, the specimen's tensile strength at the power of 50W and welding speed of 7.5 m/min is 1223 MPa which is close to the nominal strength of the SUS304H steel. The fracture did not occur at the weld bead but occurred at heat affected zone. Meanwhile, a study reported [16] that by using joint lap configuration, in a quasi-penetration, the fracture occurred at the weld bead beneath the upper specimen and above the bottom specimen. On the other hand, the fracture was at the specimen's weld bead boundary in full penetration. The specimen used was SUS304 with a thickness of 20µm. The author summarizes that the weld strength increases with the increasing power and reduces with the increasing scanning speed. Another research [17] studied that in a resistance micro-welding of 316 low-carbon vacuum melted stainless steel wires, where the manipulative variable was the input current. The study showed that with the increasing current input, the hardness value across the weld joins decreased. Therefore, the fracture in the micro tensile testing progressed as the current input increased. The study showed that a minimum current of 90A is needed to obtain a join. The highest Joint Break Force (JBF) was recorded when the current was 200A, where the JBF was 75N. Over-welding occurred when the current surpassed 350A.

IV. CONCLUSION

The SS304 thin foils and the DSS 2205 were successfully laser micro welded using pulse wave mode in the joint lap configuration. Following are the results;

- The processing parameters influence the weld geometry and the mechanical properties of the weld joint of DSS2205 and SS304.
- Specimen B possessed a weld width of 0.611mm with the power of 85%, hatching distance of 0.003mm, exhibiting tensile strength of 13.45 MPa, which is 1.7% of the DSS tensile strength.

- The specimen I possessed a weld width of 0.577mm with the parameter of power 95% and a hatching distance of 0.001mm.
- Specimen I has the weakest join strength with an average ultimate tensile strength of 0.8 MPa. This could be due to the too high power, which has distorted the weld pool resulting in a poor joint.
- Impurities development causes porosity and warp formation in the fusion zone. The highest distortion lies with specimen I, with 5.013° on the left side and 4.086° on the right side.
- When the laser power and scanning velocity surpass the optimal laser welding condition, welding defects occur in the weld bead. The higher welding intensity may be achieved in the overlap welding of ultra-thin sheets with a higher scanning velocity and smaller spot diameter.
- The focal width should be smaller than the material thickness. Laser scanning speed should be high enough to function in close proximity to incomplete penetration welding of the process boundary. The energy per unit length should be as small as possible to minimize the thermal stress to which the part is subjected.

A. Acknowledgments

The authors would like to thank the Ministry of Higher Education for providing financial support under Fundamental Research Grant Scheme (FRGS) No. FRGS/1/2021/TK0/UMP/02/22(University reference RDU210127). The authors would like to acknowledge the assistance given by Kishen A/L Manoharan.

References

[1] S. F. Haider, M. Quazi, J. Bhatti, M. N. Bashir, and I. Ali, ``Effect of Shielded Metal Arc Welding (SMAW) parame-ters on mechanical properties of low-carbon, mild and stainless-steel welded joints: A review,'' *Journal of Advances in Technology and Engineering Research*, vol. 5, no. 5, pp. 191-198, 2019. doi: https://dx.doi.org/10.20474/jater-5.5.1

[2] M. Quazi, ``An overview of laser welding of high strength steels for automotive application,'' *KA Manoharan, MM Quazi, MN Bashir, MNM Salleh, AQ Zafiuddin, and R. Linggamm,"An Overview of Laser Welding of High Strength Steels for Automotive Application", International Journal of Technology and Engineering Studies*, vol. 6, no. 1, pp. 23-40, 2020. doi: https://dx.doi.org/10.20469/ijtes.6.10004-1

[3] S. Aslanlar, ``The effect of nucleus size on mechanical properties in electrical resistance spot welding of sheets used in automotive industry,'' *Materials & Design*, vol. 27, no. 2, pp. 125-131, 2006. doi: https://doi.org/10.1016/j.matdes.2004.09.025

[4] M. Zwicker, M. Moghadam, W. Zhang, and C. Nielsen, ``Automotive battery pack manufacturing- A review of battery to tab joining,'' *Journal of Advanced Joining Processes*, vol. 1, pp. 1-37, 2020. doi: https://doi.org/10.1016/j.jajp.2020.100017

[5] E. Haddad, J. Helm, A. Olowinsky, and A. Gillner, ``Nanosecond pulsed fiber laser as a tool for laser micro welding,'' *Procedia CIRP*, vol. 94, pp. 571-576, 2020. doi: https://doi.org/10.1016/j.procir.2020.09.077

[6] M. Quazi, M. Ishak, M. Fazal, A. Arslan, S. Rubaiee, A. Qaban, M. Aiman, T. Sultan, M. Ali, and S. Manladan, ``Current research and development status of dissimilar materials laser welding of titanium and its alloys,'' *Optics & Laser Technology*, vol. 126, pp. 1-36, 2020. doi: https://doi.org/10.1016/j.optlastec.2020.106090

[7] M. Salleh, M. Ishak, M. Quazi, and M. Aiman, ``Microstructure, mechanical, and failure characteristics of laser-microwelded AZ31B Mg alloy optimized by response surface methodology,'' *The International Journal of Advanced Manufacturing Technology*, vol. 99, no. 1, pp. 985-1001, 2018. doi: https://doi.org/10.1007/s00170-018-2529-1

[8] M. M. Quazi, M. Ishak, A. Arslan, M. Fazal, F. Yusof, B. Sazzad, M. N. Bashir, and M. Jamshaid, ``Mechanical and tribological performance of a hybrid MMC coating deposited on Al-17Si piston alloy by laser composite surfacing technique,'' *RSC Advances*, vol. 8, no. 13, pp. 6858-6869, 2018. doi: https://doi.org/10.1039/C7RA08191J

[9] A. Hozoorbakhsh, M. Hamdi, A. A. D. M. Sarhan, M. I. S. Ismail, C.-Y. Tang, and G. C.-P. Tsui, ``CFD modelling of weld pool formation and solidification in a laser micro-welding process,'' *International Communications in Heat and Mass Transfer*, vol. 101, pp. 58-69, 2019. doi: https://doi.org/10.1016/j.icheatmasstransfer.2019.01.001

[10] M. Quazi, M. Ishak, M. Fazal, A. Arslan, S. Rubaiee, M. Aiman, A. Qaban, F. Yusof, T. Sultan, M. Ali *et al.*, ``A comprehensive assessment of laser welding of biomedical devices and implant materials: recent research, development and applications,'' *Critical Reviews in Solid State and Materials Sciences*, vol. 46, no. 2, pp. 109-151, 2021. doi: https://doi.org/10.1080/10408436.2019.1708701

[11] S. Wakeel, S. Bingol, M. N. Bashir, and S. Ahmad, ``Selection of sustainable material for the manufacturing of complex automotive products using a new hybrid goal programming model for best worst method--proximity indexed value method,'' *Proceedings of the Institution of Mechanical Engineers, Part L: Journal of Materials: Design and Applications*, vol. 235, no. 2, pp. 385-399, 2021. doi: https://doi.org/10.1177/1464420720966347

[12] A. Zaifuddin, M. Aiman, M. Quazi, M. Ishak, and T. Ariga, ``Effect of Laser Surface Modification (LSM) on laser energy absorption for laser brazing,'' in *IOP Conference Series: Materials Science and Engineering,* Kuantan, Malaysia, 2020.

[13] M. Haneef, M. Aiman, M. Salleh, M. Quazi, and M. Ishak, ``Microstructure analysis and mechanical properties of dissimilar AA6061-AA7075 laser brazing with prefixed ER5356 filler,'' in *IOP Conference Series: Materials Science and Engineering,* Pekan, Malaysia, 2021.

[14] M. N. M. Salleh, M. Ishak, K. Yamasaki, M. M. Quazi, and A. M. Halil, ``Pulsed nd: YAG laser parameters effect on welding uncoated Advance High Strength Steel (AHSS) for automotive,'' *Journal of Advanced Research in Fluid Mechanics and Thermal Sciences*, vol. 84, no. 1, pp. 91-100, 2021. doi: https://doi.org/10.37934/arfmts.84.1.91100

[15] M. Hummel, C. Schöler, A. Häusler, A. Gillner, and R. Poprawe, ``New approaches on laser micro welding of copper by using a laser beam source with a wavelength of 450 nm,'' *Journal of Advanced Joining Processes*, vol. 1, pp. 1-19, 2020. doi: https://doi.org/10.1016/j.jajp.2020.100012

[16] Y. Zhong, J. Xie, Y. Chen, L. Yin, P. He, and W. Lu, ``Microstructure and mechanical properties of micro laser welding NiTiNb/Ti6Al4V dissimilar alloys lap joints with nickel interlayer,'' *Materials Letters*, vol. 306, p. e130896, 2022. doi: https://doi.org/10.1016/j.matlet.2021.130896

[17] A. Das, R. Fritz, M. Finuf, and I. Masters, ``Blue laser welding of multilayered aisi 316l stainless steel micro-foils,'' *Optics & Laser Technology*, vol. 132, pp. 1-9, 2020. doi: https://doi.org/10.1016/j.optlastec.2020.106498

[18] S. Venkatesu, M. Gangaraju, S. Bhaskar, and B. V. V. Naidu, ``A study of laser beam welding, gas tungsten arc welding and high temperature brazing processes on micro hardness and tensile strength of AISI type 316 stainless steel,'' *Procedia Computer Science*, vol. 133, pp. 10-18, 2018. doi: https://doi.org/10.1016/j.procs.2018.07.003

[19] P. Woizeschke and F. Vollertsen, ``Laser keyhole micro welding of aluminum foils to lap joints even with large gap sizes,'' *CIRP Annals*, vol. 69, no. 1, pp. 237-240, 2020.